Frontiers in Bioscience Landmark

Front. Biosci. (Landmark Ed) **2023**; 28(7): 140
https://doi.org/10.31083/j.fbl2807140

Original Research

A Metabolomics-Based Study on NMDAR-Mediated Mitochondrial Damage through Calcium Overload and ROS Accumulation in Myocardial Infarction

Yuanyuan Wang[1], Li He[1,2], Dan Du[3], Zeyi Cheng[1], Chaoyi Qin[1,2,*]

[1]Department of Cardiovascular Surgery, West China Hospital, Sichuan University, 610007 Chengdu, Sichuan, China
[2]Cardiovascular Surgery Research Laboratory, West China Hospital, Sichuan University, 610007 Chengdu, Sichuan, China
[3]West China - Washington Mitochondria and Metabolism Center, West China Hospital, Sichuan University, 610007 Chengdu, Sichuan, China
*Correspondence: qinchaoyi@wchscu.cn (Chaoyi Qin)
Academic Editor: Haseeb Ahmad Khan
Submitted: 12 December 2022 Revised: 16 March 2023 Accepted: 21 March 2023 Published: 19 July 2023

Abstract

Background: Coronary artery disease is a leading public health problem. However, the mechanisms underlying mitochondrial damage remain unclear. The present study verified and explored the novel mechanisms underlying ischemic injury based on a metabolomic analysis. **Methods**: Mouse models of acute myocardial infarction were established, and serum samples were collected for targeted liquid chromatography with tandem mass spectrometry analysis. Based on metabolomic analyses, the *N*-methyl-D-aspartic acid receptor (NMDAR)–related calcium transporting signaling pathway was selected. Primary cardiomyocyte cultures were used, and *N*-methyl-D-aspartic acid (NMDA) was used as an agonist to confirm the role of NMDAR in ischemic injury. In addition, Bax, Bcl-2, mitochondrial calcium, potential, and mitochondrial reactive oxygen species accumulation were used to explore the role of NMDAR in mitochondrial damage–induced apoptosis. **Results**: Glutamate-related metabolism was significantly altered following in acute myocardial infarction. NMDA induces apoptosis under hypoxic conditions NMDAR was translocated to the mitochondrial-related membrane after activation, and its mitochondrial expression was significantly increased ($p < 0.05$). Mitochondrial damage–induced apoptosis was significantly inhibited by a selective NDMAR antagonist ($p < 0.05$), while Bax expression was remarkably decreased and Bcl-2 expression was increased ($p < 0.05$). To further explore the mechanism of NMDAR, mitochondrial calcium, membrane potential, and reactive oxygen species were detected. With NMDAR inhibition under hypoxic conditions, mitochondrial morphology and function were preserved ($p < 0.05$). **Conclusions**: Our metabolomic study identified NMDAR as a promising target. In conclusion, our study provides solid data for further studies of the role of NMDAR in cardiovascular diseases and a promising target to interfere with apoptosis in acute myocardial infarction.

Keywords: metabolomics; myocardial infarction; NMDAR; calcium overload; mitochondrial damage

1. Introduction

Coronary artery disease remains a leading public health problem in developed and developing countries [1]. Although evolutionary primary coronary intervention (PCI) significantly improves the survival of patients with acute myocardial infarction (AMI), many AMI patients do not receive PCI in the window for different reasons [2]. However, patients may still experience heart failure after revascularization of the major culprit vessels through PCI [3]. In ischemic attack, the supply of oxygen and nutrition is strictly limited [4]. A remarkable number of cardiomyocytes die because of the accumulation of free radicals, lipid peroxidation, unbalanced calcium dynamics, altered energy, mitochondrial damage, or DNA disruption [5–8]. Our previous studies mainly focused on mitochondrial damage after ischemic injury [9,10]. Mitochondria, as the energetic core of the body, play a critical role in this pathological process.

Metabolomics is an emerging "omics" science involving the comprehensive features of metabolites and metabolism in biological systems [11]. Metabolomics is a promising method for diagnosing diseases, understanding pathophysiology, exploring the inner mechanisms, identifying novel drugs and pharmacological targets, and monitoring therapeutic outcomes [12]. Therefore, the present study used metabolomics to scan metabolic changes in a AMI murine model, which provided a detailed interrogation and several findings on the altered metabolism in this model. We further verified the target key protein and explored its mechanism of action in ischemic injury.

2. Methods

2.1 Establishment of AMI Murine Model

Fifteen male 10-week-old C57BL/6 mice (Chengdu DOSSY Experimental Animals Co., Ltd., China) from the same batch were divided into a sham-control group (n = 5) and an AMI model group (n = 10). As described by Gao *et al.* [13], the mice were anesthetized with an intraperitoneal injection of ketamine (50 mg/kg) and pentobarbital sodium (50 mg/kg) without ventilation support. A small

incision was made left of the sternum, and a purse-string suture was prepared. The thorax was punctured and dilated using a mosquito clamp at the left 4th intercostal space. The beating heart was gently "popped out" and an 8-0 silk suture was quickly applied at a site on the left free wall approximately 3 mm below the atrium to block the left anterior descending coronary artery. Ligation was confirmed when the anterior left ventricular wall became pale. Following ligation, the heart was returned to the intrathoracic space and intrathoracic air was evacuated manually. The previous purse-string suture was tied and the mouse monitored during the recovery period. Mice in the sham-control group underwent the same surgical procedure and the beating hearts "popped out" without any ligation. All animal experiments were strictly performed following the National Institutes of Health Guide for the Care and Use of Laboratory Animals (Publication no. 8023, revised in 1978) and registered with the Animal Ethics Committee of West China Hospital, Sichuan University (no. 20220221020).

2.2 Sample Collections for Metabolomic Analysis

All serum samples were collected at 24 h postoperative. As in our previous study [11], each serum sample was precipitated using methanol spiked with two internal standards. The supernatant was then collected. The dried supernatant was reconstituted with 10 mM ammonium acetate in 30% water/70% acetonitrile + 0.2% acetic acid containing 12.6 µM $^{3}C_{5}$–^{15}N-L-tyrosine and 34.68 µM $^{13}C_{1}$-L-lactate.

2.3 Ultra-High-Performance Liquid Chromatography Triple Quadrupole Mass Spectrometry Data Acquisition

The final sample reconstitution was added to the ultra-high-performance liquid chromatography with tandem mass spectrometry under positive and negative ion modes. The quality control (QC) sample was set as the pooled sample with a mixture of all serum samples. The targeted metabolomics analysis was conducted using an LC-40A Ultra-Performance Liquid Chromatography (UHPLC) system coupled with an AB Sciex triple quadrupole 5500 mass spectrometer (Nexera, Framingham, MA, USA). Chromatographic separation was performed on a BEH Amide column (2.1 × 100, 1.7 µm; Waters, Milford, MA, USA) at 35 °C. The mobile phase and gradient conditions, as well as the parameters for the mass spectrometer, were described previously [11]. Multiple reaction monitoring mode was used to detect the metabolites of interest. The targeted analysis included 238 metabolites selected from over 40 metabolic pathways. The data were acquired using Analyst 1.6.3^{TM} software (AB Sciex, Framingham, MA, USA) and analyzed using Multiquant 3.0.2 software (AB Sciex, Framingham, MA, USA).

2.4 Primary Cardiomyocytes Culture and Oxygen–Glucose Deprivation Model

Myocardiocytes are isolated rat cardiomyocytes, and the cell type was further verified with IF staining of α-actinin (**Supplementary Fig. 1**). Neonatal cardiomyocytes were prepared as described previously [14]. In brief, the hearts were collected from neonatal mice within 24–48 h and cut into pieces in D-Hank's balanced salt solution. The cardiac tissues were digested in 22.5 µg/mL liberase blendzyme IV (Roche, Mannheim, Germany) at 37 °C for 40 min. Isolated cardiomyocytes in the pellet after centrifugation were resuspended in M199 medium with 10% fetal bovine serum and cultured in pre-coated plates. After 48 h, the cardiomyocytes were subjected to various treatments and measurements after 48 h of culture.

The oxygen–glucose deprivation (OGD) model was defined as a glucose-free medium under a deoxygenated atmosphere. In the present study, the OGD model was set with no glucose and 0% oxygen for 6 h of treatment before the sample collection.

NMDA (HY-17551; MedChemExpress, NJ, USA) was used as an agonist of NMDAR. NMDA was administered 30 min before the ODG or normoxic condition. In the preliminary study, NMDA concentrations were set at 10 µM, 50 µM, and 100 µM, and the final working dose was 10 µM. MK-801 (HY-15084B; MedChemExpress), which was used as a selective NMDAR antagonist, was preadministered for 30 min at a concentration of 10 µM.

2.5 Western Blot Analysis

Cardiomyocyte lysates were subjected to western blotting analysis. Specific target proteins (Caspase-3, NMDAR1A, Bax, and Bcl-2) were separated from the cell lysates, transferred to polyvinylidene difluoride membranes, and visualized by chemiluminescence. The primary antibodies included rabbit anti-α-tubulin (bs-0159R; Bioss, Bejing, China), rabbit anti-cleaved-caspase 3 and caspase 3 (ab214430 and ab184787; Abcam, Cambridge, England), rabbit anti-Bax (ab182734; Abcam), rabbit anti-Bcl-2 (ab18258; Abcam), and mouse anti-NMDAR1A (32-0500; Thermo Fisher Scientific, Cleveland, OH, USA).

2.6 RNA Extraction and Quantitative Real-Time Polymerase Chain Reaction

Total RNA from cultured cardiomyocytes was extracted using TRIzol reagent (Sigma, Poole, Dorset, UK). Circular DNA was synthesized using M-MLV reverse transcriptase (Invitrogen, Burlington, IA, USA). SYBR Green PCR master mix was used according to the manufacturer's instructions (Eurogentec, San Diego, CA, USA), while 28S rRNA was used as a loading control. The primer sequences were as follows: nmdar1a 5′-ACT TGA AGG GCT TGG AGA-3′ (forward) and 5′-GGA GTG GAA CGG AAT GAT-3′ (reverse); nmdar2b 5′-GCT GGA GGC GTT GGA TGT-3′ (forward) and 5′-AAT GTG GAT TGG GAG GAC-3′ (re-

verse); 28S rRNA 5′-TTG AAA ATC CGG GGG AGA G-3′ (forward) and 5′-ACA TTG TTC CAA CAT GCC AG-3′ (reverse). A total of 34 amplification cycles were conducted on an Eppendorf Real-Time PCR machine. The expression of nmdar1a/nmdar2b in relation to the 28S rRNA control was determined.

2.7 Transmission Electron Microscope

The samples were fixed with 3% glutaraldehyde for 24 h, fixed in 1% osmium tetroxide, dehydrated in a series of acetone, infiltrated in Epon 812 for 30–60 min each time, and finally embedded. The semi-thin sections were stained with methylene blue, and ultrathin sections were cut with a diamond knife and stained with uranyl acetate and lead citrate. The sections were examined using a transmission electron microscopy (TEM, JEM-1400 Flash, JEOL Ltd., Tokyo, Japan).

2.8 Cell Counting Kit-8 Assay

A cell counting kit-8 (CCK-8) assay kit was purchased from Dojindo (Dojindo Molecular Technologies, Inc., Kumamoto, Japan). Cardiomyocytes were cultured in 96-well plates according to the manufacturer's instructions. Following the different treatments, 10 µL of CCK-8 solution was added to each well. After 2 h of incubation, the absorbance was measured at 450 nm by a microplate reader.

2.9 Mitochondrial Measurements

Calcium concentration (ab142780; Abcam), mitochondrial ROS (M36008; Thermo Fisher Scientific), and mitochondrial membrane potential (M34152; Thermo Fisher Scientific) were measured using specific assay kits according to the manufacturer's instructions.

2.10 Statistical Analysis

The statistical analysis was performed using SPSS software version 19 (SPSS Inc., Chicago, IL, USA). The results are presented as mean ± standard error of the mean (SEM). The data were analyzed using one-way analysis of variance, followed by the Bonferroni post-hoc test. An unpaired Student's *t*-test was used to compare groups. Statistical significance was set at $p < 0.05$.

3. Results

3.1 Metabonomic Changes in Response to AMI in Murine Model

To identify the altered profiles of metabolites in myocardial infarction, a targeted liquid chromatography with tandem mass spectrometry comprehensive analysis of 238 metabolites in positive and negative modes was performed on serum samples. A principal component analysis indicated that the metabolic profiles of mice in the AMI groups deviated from those of the sham-control group, showing alterations in metabolism profiles in AMI (Fig. 1).

3.2 Pathway Analysis of Serum Sample from AMI Murine Model

A heat map is shown in Fig. 2A. The most affected pathways were identified according to the Kyoto Encyclopedia of Genes and Genomes signaling pathway analysis based on the metabolites (impact values >0.2), including: (1) D-glutamine and D-glutamate metabolism; (2) alanine, aspartate, and glutamate metabolism; and (3) taurine and hypotaurine metabolism (Fig. 2B). Several metabolites involved in these signaling pathways are shown in Fig. 3 ($p < 0.0001$).

3.3 NMDAR Participates in Ischemic Injury–Induced Cardiomyocytes Apoptosis

According to the metabolomics results, glutamate was selected as an essential excitatory neurotransmitter, which reportedly exerts multiple regulatory effects through its specific ligand (*N*-methyl-D-aspartic acid receptor [NMDAR]) [15]. Thus, to confirm the role of NMDAR in ischemic injury–induced cardiomyocyte apoptosis, we performed further studies in cell culture. NMDA is a highly selective agonist of NMDAR. Different doses (10 µM, 50 µM, and 100 µM) of NMDA were used for pre-treatment for 30 min. As shown in Fig. 4A, NMDA did not exert any adverse effects under normal conditions ($p > 0.05$). Hypoxic injury–induced cell death and NMDA aggravated hypoxic injury in a dose-dependent manner ($p < 0.05$). We also detected significantly elevated expression of cleaved caspase 3 under hypoxic injury ($p < 0.05$). After NMDA treatment, cleaved caspase 3 levels were further increased ($p < 0.05$; Fig. 4B). Surprisingly, the mRNA levels of NMDAR were similar under normal and hypoxic conditions ($p > 0.05$; Fig. 4C). Therefore, mitochondrial proteins were extracted, and we found enriched NMDAR expression in the mitochondria under hypoxic injury ($p < 0.05$; Fig. 4D).

3.4 NMDAR-Mediated Mitochondrial Damage Induces Cardiomyocyte Apoptosis

Given the translocation of NMDAR into the mitochondria under hypoxic injury, we further explored NMDAR-mediated mitochondrial damage in hypoxic injury–induced apoptosis. MK-801, a selective NMDAR antagonist, was administered. With NMDAR inhibition, apoptosis under hypoxic injury was significantly blocked, and the CCK-8 assay showed improved cell viability ($p < 0.05$; Fig. 5A,B). Bax and Bcl-2 are the two key factors involved in mitochondrial damage–induced apoptosis. Similar to the expression of cleaved caspase 3, the inhibition of NMDAR significantly decreased Bax expression and increased Bcl-2 expression under hypoxia and hypoxia with NMDA ($p < 0.05$; Fig. 5C). Transmission electron microscopy images showed normal mitochondrial morphology under normal conditions, disrupted vesicular mitochondria under hypoxia, and significant vesicular and swollen mitochondria under hypoxia and NMDA treatment. With

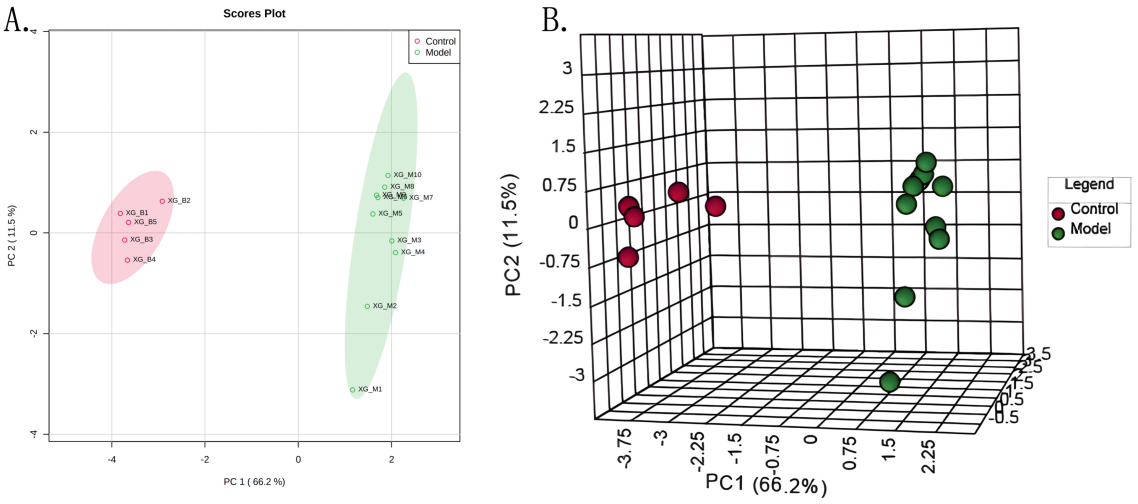

Fig. 1. PCA Scores plot (A) and 3D scores plot (B) for control and model groups. Abbreviations: PC1, principle component 1; PC2, principle component 2.

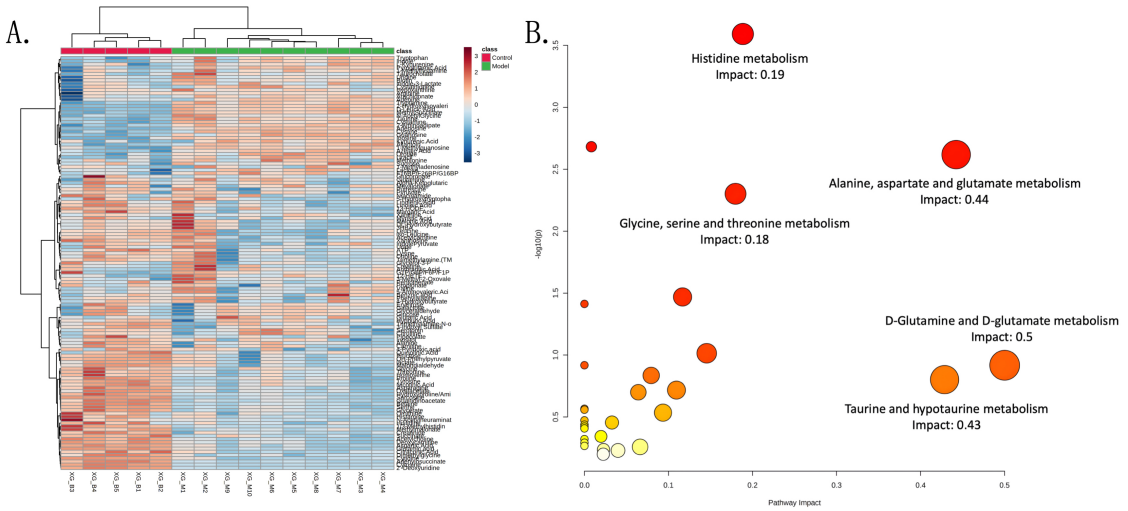

Fig. 2. Heatmap and impact pathways. (A) Heatmap of 128 metabolites in control and model groups. The colour bar from blue to red represents low to high mean intensity after normalization using the Z-score. (B) KEGG pathway analysis on the metabolites of two groups. The bubble diagram displayed selected pathways with an impact value larger than 0.2. The size of the bubbles represented impact values ranging from 0.2 to 1.0, and the colour of the bubbles means the *p* value after the negative Log transform.

MK-801 treatment, less vesicular and less swollen mitochondria were observed (Fig. 5D).

3.5 NMDAR Promotes Calcium and Mitochondrial ROS Accumulation

Calcium accumulation or overload is an essential phenomenon in ischemic injuries. The Rhod-2 calcium indicator was used to detect calcium levels in mitochondria under different circumstances. Fluorescent images showed remarkable calcium accumulation under hypoxic and non-hypoxic conditions with NMDA. Treatment with MK-801 significantly reduced mitochondrial calcium accumulation in cardiomyocytes ($p < 0.05$; Fig. 6A,B). In addition, loss of mitochondrial membrane potential was observed in hypoxia and hypoxia with NMDA conditions, while the inhibition of NMDAR restored the mitochondrial membrane potential ($p < 0.05$; Fig. 6C). Mitochondrial ROS (mitoROS) levels were measured (Fig. 6D–F); MK-801 significantly inhibited mitoROS formation ($p < 0.05$).

4. Discussion

In the present study, serum from AMI mice was subjected to liquid chromatography with tandem mass spectrometry–based metabolomic analysis, which showed significantly disturbed metabolic pathways and metabolite alterations. With further analysis, a glutamate-related metabolism pathway was identified in the process of AMI and NMDAR as a calcium channel, and its role in AMI was further explored.

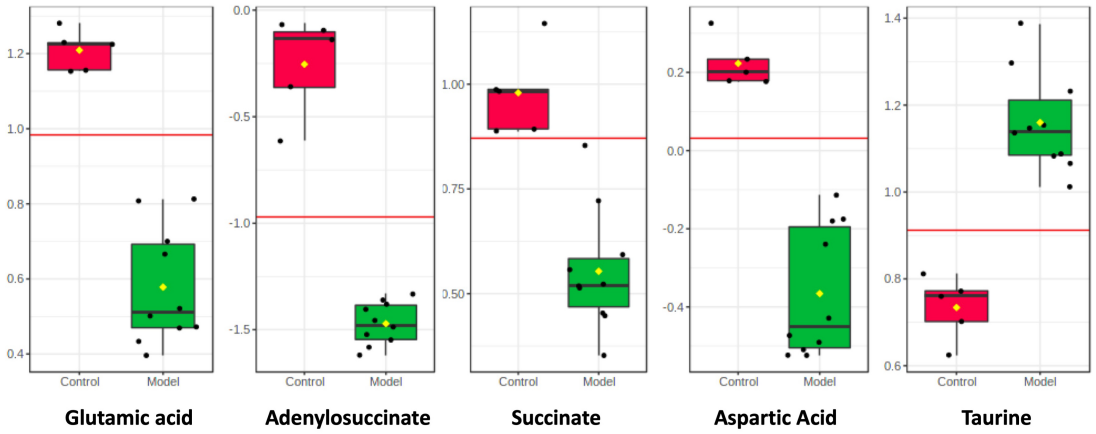

Fig. 3. Box plots showing integrated intensities for 5 selected LC-MS-identified biomarkers in two groups. The black dots represent the concentrations of the selected feature from all samples. *t*-test was used to identify the difference.

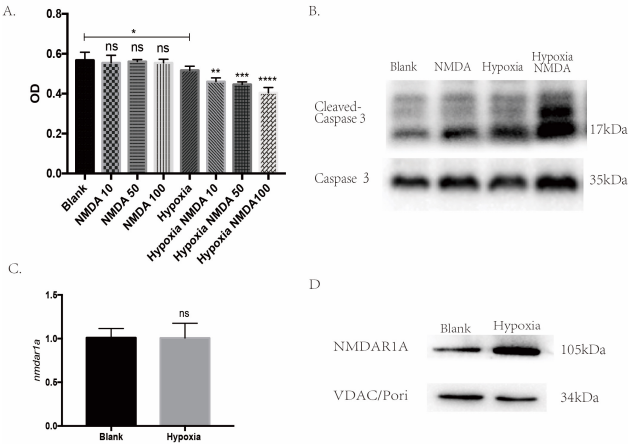

Fig. 4. NMDAR participates in the ischemic injury-induced cardiomyocyte apoptosis. (A) CCK-8 assay showed NMDA could aggravate the hypoxic injury in a dose-dependent manner (*$p < 0.05$ *vs.* Blank; **$p < 0.01$ *vs.* Blank; ***$p < 0.001$ *vs.* Blank; ****$p < 0.0001$ *vs.* Blank; n = 5) while NMDA did not exert any adverse effects under normoxia (ns $p > 0.05$). (B) NMDA significantly increased the level of cleaved caspase-3 under hypoxia ($p < 0.05$ *vs.* Blank; n = 5). (C) mRNA level of NMDAR showed no difference ($p > 0.05$ *vs.* Blank; n = 5). (D) The protein level of NMDAR in mitochondria showed significant elevation under hypoxic injury ($p < 0.05$ *vs.* Blank; n = 5). ns, not significant.

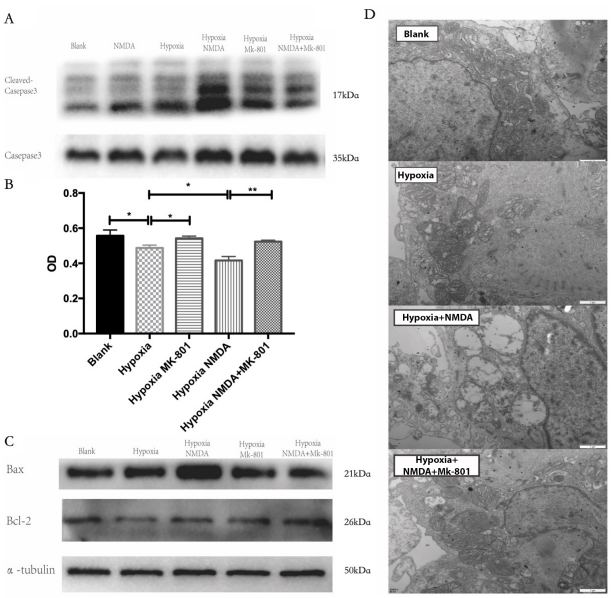

Fig. 5. NMDAR-mediated mitochondrial damage induces cardiomyocyte apoptosis. (A,B) Inhibition of NMDAR with MK-801 significantly limited apoptosis and improved survival (*$p < 0.05$; **$p < 0.01$, n = 5). (C) The protein level of Bax was inhibited with treatment of MK-801 and the Bcl-2 level was increased ($p < 0.05$ *vs.* Hypoxia, n = 5). (D) The transmission electron microscope showed mitochondria in different conditions. vesicular, disrupted mitochondria under hypoxia; significant vesicular and swollen mitochondria under hypoxia and NMDA treatment; less vesicular and less swollen mitochondria under hypoxia and MK-801.

As an emerging metabolomics technology, many studies have examined patients with AMI or AMI in animal models [16,17]. However, given the high sensitivity of metabolomic analyses, intragroup consistency has been difficult in many studies, particularly human studies. In our study, the C57BL/6 mouse strain was chosen since it has a genome-stable background. A novel and efficient mouse model of left anterior descending artery ligation–induced AMI, first reported by Gao *et al.* [13], was used to ensure that all mice in the same group were derived from the same batch and established under the same conditions. Additionally, serum samples were used instead of cardiac tissue. The area supplied by the culprit vessels was difficult to identify, and normal cardiac tissue may significantly affect

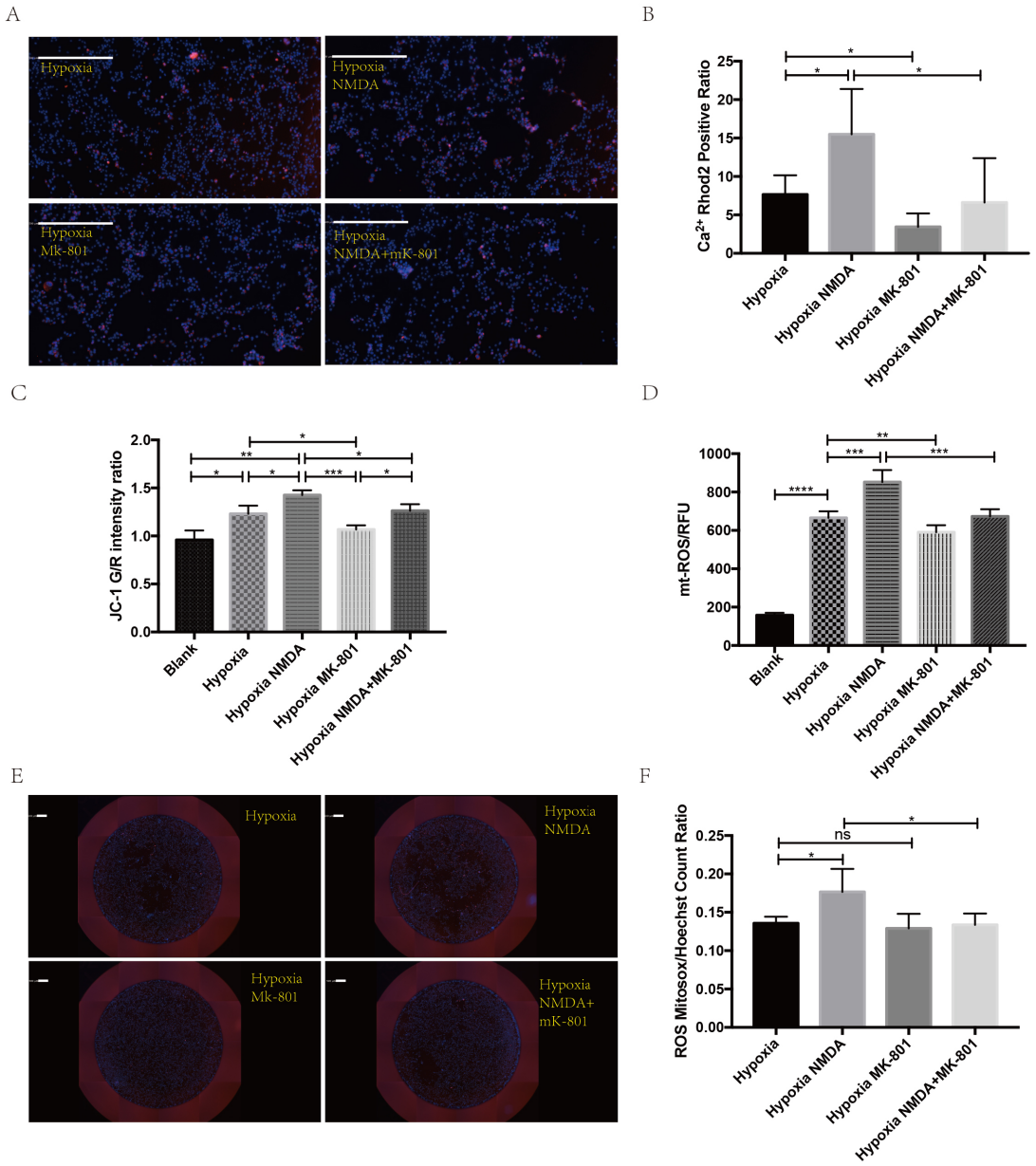

Fig. 6. NMDAR promotes calcium and mitoROS accumulation in the mitochondria. (A,B) Representative images of calcium indicator and quantification showed less calcium accumulation after MK-801 treatment (white bar =500 µm; *$p < 0.05$, n = 5). (C) Loss of mitochondrial membrane potential was identified in both hypoxia and hypoxia with NMDA, and inhibition of NMDAR could restore the mitochondrial membrane potential (*$p < 0.05$; **$p < 0.01$; ***$p < 0.001$). (D–F) Representative images of mitochondrial ROS accumulation and quantification showed inhibition of mitoROS accumulation after MK-801 treatment (white bar =500 µm; *$p < 0.05$; **$p < 0.01$; ***$p < 0.001$; ****$p < 0.0001$; ns $p > 0.05$; n = 5).

the metabolomic results. Therefore, as shown in our results section, 10 samples from the model group and five from the control group had good consistency, which ensured the validity of further metabolic pathway analyses.

The impact of the pathways was analyzed by pathway analysis using MetaboAnalyst 5.0 (http://www.metaboanalyst.ca) to evaluate their importance after AMI. Among them, glutamate and taurine metabolism are involved in the pathological changes associated with AMI. Taurine is a sulfur amino acid present in cardiomyocytes at high concentrations. It is well known that taurine exerts antioxidative activity, protects mitochondria, and inhibits calcium overload [18–20]. More importantly, taurine can modulate calcium channels to reduce calcium overload [21].

Glutamate has multiple cellular functions, including antioxidative, pro-inflammatory, and membrane stabilization [22]. Many metabolites are synthesized from glutamate, which serves as a precursor for amino acid

biosynthesis. Moreover, the excitatory neurotransmitter (*N*-acetyl-L-aspartyl-L-glutamate) and inhibitory neurotransmitter (γ-aminobutyrate) are synthesized from glutamate, as is the antioxidant glutathione [23]. Glutamate is also involved in various signaling pathways by interacting with many membrane-bound inotropic glutamate receptors, such as NMDA and α-amino-3-hydroxy-5-methyl-4-isoazolepropionic acid [24]. Consistent with other studies [1,22], significantly impacted metabolic pathways are related to calcium transportation. NMDAR have been well-studied in the neural system, and their prolonged activation could result in Ca^{2+}-dependent neurotoxicity. NMDAR activation has high permeability to extracellular Ca^{2+} and Na^{+} and causes a rapid increase in intracellular Ca^{2+}, triggering various signaling pathways of cell death [15,25]. According to our metabolomic analysis, NMDAR may play an essential role in modulating Ca^{2+} homeostasis under ischemic stress in cardiomyocytes. Few studies have reported the role of NMDAR in heart disease.

NMDAR was recently reported in the cardiovascular system, and its extensive activation drives calcium influx to promote ischemic injury or ischemia–reperfusion injury [26–30]. Liu *et al*. [28] reported that NMDA could promote calcium influx and calcium-channel blockers could rescue NMDAR-induced apoptosis through the p38 MAPK signaling pathway.

In the present study, we identified the effects of NMDAR activation under normoxic and hypoxic conditions. NMDA-stimulated NMDAR showed no difference in cell death under normoxic conditions, whereas NMDA showed significant adverse effects on hypoxic cardiomyocytes. In addition, under hypoxic conditions, no significant difference in NMDAR mRNA levels was found, a finding that was inconsistent with Hu's research [29]. However, we observed significantly higher mitochondrial protein levels. Therefore, we hypothesized that NMDAR might translocate to the mitochondrial membrane to transport calcium under hypoxic stress.

Mitochondrial damage–induced apoptosis is a classic cell death pathway in ischemic heart disease [31]. Calcium overload and ROS accumulation in the mitochondria are two key pathological milestones in ischemic injury [32]. The present study was the first to identify mitochondrial damage and alterations in related signaling pathways. NMDA significantly deteriorated mitochondrial damage and apoptosis, whereas MK-801 inhibited NMDAR-mediated mitochondrial damage and apoptosis. Furthermore, the measurement of intracellular calcium, mitoROS, and mitochondrial potential revealed the detailed adverse effects of NDMAR on mitochondrial damage and apoptosis.

Although our study presented the metabolomic results of a highly consistent myocardial infarct mouse model and a promising target based on this metabolomic analysis, it has some limitations. First, only cellular studies were performed to explore the mechanism. Primary cardiomyocytes and a classic OGD cell model were used to mimic myocardial infarction. The mechanism will be further tested in animal models in our lab. Second, the translocation of NMDAR from the endoplasm to the mitochondrial or mitochondria-associated endoplasmic reticulum membranes requires confirmation. Overall, NMDAR, as a functional receptor in the neural system, requires further exploration in the cardiovascular system.

5. Conclusions

Here we reported the results of our metabolomics study using a highly consistent myocardial infarction mouse model. According to a metabolomic study, NMDAR was identified as a promising target that could induce mitochondrial damage and cell apoptosis by mediating calcium influx and ROS formation. In conclusion, our study provides solid data for further study of the role of NMDAR in cardiovascular diseases and a promising target to interfere with apoptosis in myocardial infarction.

Availability of Data and Materials

The datasets used and/or analyzed during the currentstudy are available from the corresponding author upon reasonable request.

Author Contributions

YW and LH performed most experiments. DD and ZC performed metabolic experiments. YW performed computational data analyses. CQ provided samples. CQ contributed protocols, made some constructs, and provided consultation. CQ established collaborations and allocated funding for this study. All authors contributed to editorial changes in the manuscript. All authors read and approved the final manuscript. All authors have participated sufficiently in the work to take public responsibility for appropriate portions of the content and agreed to be accountable for all aspects of the work in ensuring that questions related to its accuracy or integrity.

Ethics Approval and Consent to Participate

All animal work was registered in the ethical committee of Sichuan University (No. 20220221020) and strictly performed following the National Institutes of Health guide for the care and use of Laboratory animals (NIH Publications No. 8023, revised 1978).

Acknowledgment

Not applicable.

Funding

The present study was financially supported by the National Natural Science Foundation of China (Grant No. 81900311) and the Science and Technology Agency Foundation of Sichuan province (Grant 2022YFS0364).

Conflict of Interest

The authors declare no conflict of interest.

Supplementary Material

Supplementary material associated with this article can be found, in the online version, at https://doi.org/10.31083/j.fbl2807140.

References

[1] Liu YT, Zhou C, Jia HM, Chang X, Zou ZM. Standardized Chinese Formula Xin-Ke-Shu inhibits the myocardium Ca(2+) overloading and metabolic alternations in isoproterenol-induced myocardial infarction rats. Scientific Reports. 2016; 6: 30208.

[2] Menees DS, Peterson ED, Wang Y, Curtis JP, Messenger JC, Rumsfeld JS, *et al*. Door-to-balloon time and mortality among patients undergoing primary PCI. The New England Journal of Medicine. 2013; 369: 901–909.

[3] Hausenloy DJ, Yellon DM. Targeting Myocardial Reperfusion Injury–The Search Continues. The New England Journal of Medicine. 2015; 373: 1073–1075.

[4] Prabhat AM, Kuppusamy ML, Naidu SK, Meduru S, Reddy PT, Dominic A, *et al*. Supplemental Oxygen Protects Heart Against Acute Myocardial Infarction. Frontiers in Cardiovascular Medicine. 2018; 5: 114.

[5] Chen X, Li X, Xu X, Li L, Liang N, Zhang L, *et al*. Ferroptosis and cardiovascular disease: role of free radical-induced lipid peroxidation. Free Radical Research. 2021; 55: 405–415.

[6] Li Y, Zhang Z, Li S, Yu T, Jia Z. Therapeutic Effects of Traditional Chinese Medicine on Cardiovascular Diseases: the Central Role of Calcium Signaling. Frontiers in Pharmacology. 2021; 12: 682273.

[7] Guo Z, Fan D, Liu FY, Ma SQ, An P, Yang D, *et al*. NEU1 Regulates Mitochondrial Energy Metabolism and Oxidative Stress Post-myocardial Infarction in Mice *via* the SIRT1/PGC-1 Alpha Axis. Frontiers in Cardiovascular Medicine. 2022; 9: 821317.

[8] Fu W, Ren H, Shou J, Liao Q, Li L, Shi Y, *et al*. Loss of NPPA-AS1 promotes heart regeneration by stabilizing SFPQ-NONO heteromer-induced DNA repair. Basic Research in Cardiology. 2022; 117: 10.

[9] Qin C, Wu XL, Gu J, Du D, Guo Y. Mitochondrial Dysfunction Secondary to Endoplasmic Reticulum Stress in Acute Myocardial Ischemic Injury in Rats. Medical Science Monitor. 2020; 26: e923124.

[10] Qin CY, Zhang HW, Gu J, Xu F, Liang HM, Fan KJ, *et al*. Mitochondrial DNA induced inflammatory damage contributes to myocardial ischemia reperfusion injury in rats: Cardioprotective role of epigallocatechin. Molecular Medicine Reports. 2017; 16: 7569–7576.

[11] Huang Y, Wen Y, Wang R, Hu L, Yang J, Yang J, *et al*. Temporal metabolic trajectory analyzed by LC-MS/MS based targeted metabolomics in acute pancreatitis pathogenesis and Chaiqin Chengqi decoction therapy. Phytomedicine. 2022; 99: 153996.

[12] Long NP, Nghi TD, Kang YP, Anh NH, Kim HM, Park SK, *et al*. Toward a Standardized Strategy of Clinical Metabolomics for the Advancement of Precision Medicine. Metabolites. 2020; 10: 51.

[13] Gao E, Lei YH, Shang X, Huang ZM, Zuo L, Boucher M, *et al*. A novel and efficient model of coronary artery ligation and myocardial infarction in the mouse. Circulation Research. 2010; 107: 1445–1453.

[14] Wu Y, Qin C, Lu X, Marchiori J, Feng Q. North American ginseng inhibits myocardial NOX2-ERK1/2 signaling and tumor necrosis factor-α expression in endotoxemia. Pharmacological Research. 2016; 111: 217–225.

[15] Bakaeva Z, Goncharov M, Krasilnikova I, Zgodova A, Frolov D, Grebenik E, *et al*. Acute and Delayed Effects of Mechanical Injury on Calcium Homeostasis and Mitochondrial Potential of Primary Neuroglial Cell Culture: Potential Causal Contributions to Post-Traumatic Syndrome. International Journal of Molecular Sciences. 2022; 23: 3858.

[16] Li J, Duan W, Wang L, Lu Y, Shi Z, Lu T. Metabolomics Study Revealing the Potential Risk and Predictive Value of Fragmented QRS for Acute Myocardial Infarction. Journal of Proteome Research. 2020; 19: 3386–3395.

[17] Wu G, Zhong J, Chen L, Gu Y, Hong Y, Ma J, *et al*. Effects of the Suxiao Jiuxin pill on acute myocardial infarction assessed by comprehensive metabolomics. Phytomedicine: International Journal of Phytotherapy and Phytopharmacology. 2020; 77: 153291.

[18] Yang YJ, Han YY, Chen K, Zhang Y, Liu X, Li S, *et al*. TonEBP modulates the protective effect of taurine in ischemia-induced cytotoxicity in cardiomyocytes. Cell Death & Disease. 2015; 6: e2025.

[19] Shimada-Takaura K, Takahashi K, Ito T, Schaffer S. Role for Taurine in Development of Oxidative Metabolism After Birth. Advances in Experimental Medicine and Biology. 2017; 975 Pt 2: 1047–1057.

[20] Ren F, Liu X, Liu X, Cao Y, Liu L, Li X, *et al*. *In vitro* and *in vivo* study on prevention of myocardial ischemic injury by taurine. Annals of Translational Medicine. 2021; 9: 984.

[21] Wang J, Qi C, Liu L, Zhao L, Cui W, Tian Y, *et al*. Taurine Protects Primary Neonatal Cardiomyocytes Against Apoptosis Induced by Hydrogen Peroxide. International Heart Journal. 2018; 59: 190–196.

[22] Yang Y, Jia H, Yu M, Zhou C, Sun L, Zhao Y, *et al*. Chinese patent medicine Xin-Ke-Shu inhibits Ca^{2+} overload and dysfunction of fatty acid β-oxidation in rats with myocardial infarction induced by LAD ligation. Journal of Chromatography. B, Analytical Technologies in the Biomedical and Life Sciences. 2018; 1079: 85–94.

[23] Yelamanchi SD, Jayaram S, Thomas JK, Gundimeda S, Khan AA, Singhal A, *et al*. A pathway map of glutamate metabolism. Journal of Cell Communication and Signaling. 2016; 10: 69–75.

[24] Hansen KB, Yi F, Perszyk RE, Furukawa H, Wollmuth LP, Gibb AJ, *et al*. Structure, function, and allosteric modulation of NMDA receptors. The Journal of General Physiology. 2018; 150: 1081–1105.

[25] Furuta T, Nakagawa I, Yokoyama S, Morisaki Y, Saito Y, Nakase H. Melatonin-Induced Postconditioning Suppresses NMDA Receptor through Opening of the Mitochondrial Permeability Transition Pore via Melatonin Receptor in Mouse Neurons. International Journal of Molecular Sciences. 2022; 23: 3822.

[26] Stojic I, Srejovic I, Zivkovic V, Jeremic N, Djuric M, Stevanovic A, *et al*. The effects of verapamil and its combinations with glutamate and glycine on cardiodynamics, coronary flow and oxidative stress in isolated rat heart. Journal of Physiology and Biochemistry. 2017; 73: 141–153.

[27] Liu ZY, Hu S, Zhong QW, Tian CN, Ma HM, Yu JJ. N-Methyl-D-Aspartate Receptor-Driven Calcium Influx Potentiates the Adverse Effects of Myocardial Ischemia-Reperfusion Injury Ex Vivo. Journal of Cardiovascular Pharmacology. 2017; 70: 329–338.

[28] Liu ZY, Zhong QW, Tian CN, Ma HM, Yu JJ, Hu S. NMDA receptor-driven calcium influx promotes ischemic human cardiomyocyte apoptosis through a p38 MAPK-mediated mechanism. Journal of Cellular Biochemistry. 2019; 120: 4872–4882.

[29] Hu F, Zhang S, Chen X, Fu X, Guo S, Jiang Z, *et al*. MiR-219a-2 relieves myocardial ischemia-reperfusion injury by reducing calcium overload and cell apoptosis through HIF1α/ NMDAR pathway. Experimental Cell Research. 2020; 395: 112172.

[30] Liu Y, Luo Z, Liao Z, Wang M, Zhou Y, Luo S, *et al*. Effects of Excessive Activation of N-methyl-D-aspartic Acid Receptors in Neonatal Cardiac Mitochondrial Dysfunction Induced by Intrauterine Hypoxia. Frontiers in Cardiovascular Medicine. 2022; 9: 837142.

[31] Yang H, Xue W, Ding C, Wang C, Xu B, Chen S, *et al*. Vitexin Mitigates Myocardial Ischemia/Reperfusion Injury in Rats by Regulating Mitochondrial Dysfunction via Epac1-Rap1 Signaling. Oxidative Medicine and Cellular Longevity. 2021; 2021: 9921982.

[32] Ramachandra CJA, Hernandez-Resendiz S, Crespo-Avilan GE, Lin YH, Hausenloy DJ. Mitochondria in acute myocardial infarction and cardioprotection. EBioMedicine. 2020; 57: 102884.